SCIENTIFIC REPORTS

OPEN

SUBJECT AREAS:
DRUG DELIVERY
CNS CANCER
BIOMEDICAL MATERIALS
CANCER MICROENVIRONMENT

Received
11 June 2013

Accepted
12 August 2013

Published
28 August 2013

Correspondence and requests for materials should be addressed to Z.Q.P. (zqpang@fudan.edu.cn) or X.G.J. (xgjiang@shmu.edu.cn)

Ligand modified nanoparticles increases cell uptake, alters endocytosis and elevates glioma distribution and internalization

Huile Gao, Zhi Yang, Shuang Zhang, Shijie Cao, Shun Shen, Zhiqing Pang & Xinguo Jiang

Key Laboratory of Smart Drug Delivery (Fudan University), Ministry of Education; School of Pharmacy, Fudan University; 826 Zhangheng Road, Shanghai, 201203, China.

Nanoparticles (NPs) were widely used in drugs/probes delivery for improved disease diagnosis and/or treatment. Targeted delivery to cancer cells is a highly attractive application of NPs. However, few studies have been performed on the targeting mechanisms of these ligand-modified delivery systems. Additional studies are needed to understand the transport of nanoparticles in the cancer site, the interactions between nanoparticles and cancer cells, the intracellular trafficking of nanoparticles within the cancer cells and the subcellular destiny and potential toxicity. Interleukin 13 (IL-13) peptide can specifically bind IL-13Rα2, a receptor that is highly expressed on glioma cells but is expressed at low levels on other normal cells. It was shown that the nanoparticels modification with the IL-13 peptide could improve glioma treatment by selectively increasing cellular uptake, facilitating cell internalization, altering the uptake pathway and increasing glioma localization.

Nanoparticles (NPs) are widely used in delivering drugs, genes and probes for the diagnosis and treatment of various diseases[1,2]. Active targeting strategy was developed to improve the delivery efficiency through decorating with specific ligands targeting specific receptors that were over-expressed on the diseased cells[3–5]. Using tumors as models, active nanoscale tumor targeting drug delivery systems have led to a variety of outcomes, including elevated tumor cell uptake *in vitro*, enhanced tumor targeting, improved cancer bearing survival time, and reduced side-effects *in vivo*[4,6–9]. One successful example, doxorubicin-loaded targeted polymeric NPs (BIND-014), is currently under clinical evaluation[10]. However, the interaction of these systems with targeted cells or tissues have not yet been well addressed, and several basic concerns remain: (1) What is the difference between the mechanism of tumor cell internalization of targeted NPs and non-targeted NPs? (2) Is there a significant difference in tumor localization between targeted NPs and non-targeted NPs? (3) Are there significant differences in cellular selectivity between targeted nanoparticles and non-targeted nanoparticles in the tumor site? (4) Is the targeting effect of targeting nanoparticles caused by specific recognition and enhanced internalization by tumor cells or by elevated endocytosis of macrophages in the tumor site[11]?

Interleukin 13 (IL-13) peptide can bind specifically and with high affinity to IL-13Rα2, a tumor-specific receptor overexpressed in glioma, and has demonstrated great potential for glioma targeting[12–15]. In this study, IL-13 peptide was conjugated to NPs to form a glioma targeting drug delivery system (ILNPs), which was used as a model to elucidate cancer targeting mechanisms of ligand-modified nanoparticles (Figure 1a). The fluorescent dye coumarin-6 was encapsulated into NPs and ILNPs to track the particles inside cells. Quantitative cellular uptake was performed on both U87 (a glioma cell line that highly expressed IL-13Rα2) and Raw246.7 (a macrophage cell line with low IL-13Rα2 expression) cells (Figure 1b, original data see Supplementary Fig. S1 online) to reveal the effect of ligand modification on cellular uptake. Endosomes were marked by Lysotracker Red to elucidate the participation of endosomes in the internalization process of NPs and ILNPs. Several inhibitors of cellular uptake were used to evaluate the involvement of different endocytosis pathways and the differences between NPs and ILNPs. Transmission electron microscopy (TEM) was used to directly observe the endocytosis pathways involved in the cellular uptake of superparamagnetic iron oxide (SPIO, 15 nm)-loaded ILNPs.

For *in vivo* evaluation, the near-infrared fluorescent dye DiR was loaded into NPs and ILNPs. The whole body distribution and glioma localization were evaluated by *in vivo* and *ex vivo* imaging. Brain slices were prepared and

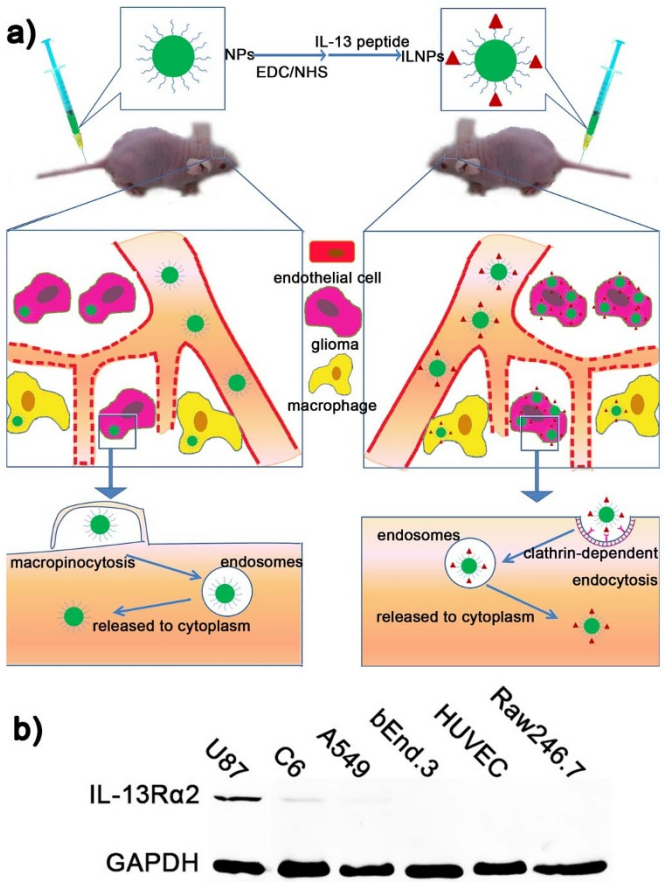

Figure 1 | Elucidation of the study. (a) Elucidation of cancer targeting mechanisms of ligand-modified NPs. IL-13 peptide modification increases glioma distribution, selectively elevates internalization by glioma cells rather than macrophages and microvessels, and changes the dominant internalization pathway from macropinocytosis to receptor-mediated clathrin-dependent endocytosis. The photos and images shown were produced by Dr Huile Gao. (b) IL-13Rα2 expression in various cells including U87, Raw246.7, HUVEC (human umbilical vein endothelial cells), bEnd.3 (cell line used as brain microvessel endothelial cells), A549 (human non-small-cell lung carcinoma cell line) and C6 (rat glioma cell line). Full length original picture can be found as Supplementary Fig. S1.

glioma cells, macrophages and microvessels were stained to further determine the difference in cell selectivity in the glioma site between NPs and ILNPs.

Results

Characterization of NP. The mean particle sizes, polydispersity index (PDI) and zeta potentials of the NPs and ILNPs were reported in Supplementary Table S1 online. Particle sizes were mostly between 100 nm to 125 nm and were narrowly distributed. Conjugation with the IL-13 peptide slightly changed the particle sizes and zeta potentials of nanoparticles. The morphology of ILNPs was spherical as demonstrated by TEM, while SPIO was loaded in the core of the ILNPs (see Supplementary Fig. S2 online). Both NPs and ILNPs were stable in phosphate buffered saline (PBS), as evidenced by the lack of obvious increases in either particle size or PDI during a 7-day long experiment (see Supplementary Fig. S2 online). Adding fetal bovine serum (FBS) to incubation medium could lead to protein adsorption on particles. However, no obvious difference was observed between NPs and ILNPs (see Supplementary Fig. S2 online), suggesting that modification with the IL-13 peptide did not significantly affect the stability of the particles. The encapsulation efficiency of DTX was 47.8% and the drug loading capacity was 1.59%[16]. The 24-h cumulative release percentages of both coumarin-6 and DiR from NPs or ILNPs were lower than 0.1%. Thus, these two probes could be utilized for the tracking of in vitro and in vivo behavior of NPs and ILNPs.

Anti-glioma effect. Although the IL-13 peptide exhibited excellent properties amenable to glioma targeting and higher glioma cell uptake was observed for nanocarriers anchored with IL-13 peptide[14,17], the anti-glioma effect of the IL-13 peptide modified drug delivery system remained unclear. In this study, the model drug docetaxel (DTX) was loaded into NPs and ILNPs. Treatment with different DTX formulations significantly prolonged the median survival time of glioma bearing mice (Figure 2a). The control mice started dying on day 21, and all of the mice died during the following 9 days. Administering free DTX delayed death but it was not obvious, which was mainly due to the systemic distribution of DTX. Encapsulation of DTX into NPs further prolonged the median survival time of mice, from 30 days for the DTX group to 35 days. DTX-ILNPs exhibited the best anti-glioma activity, which was significantly better than those of saline, DTX and

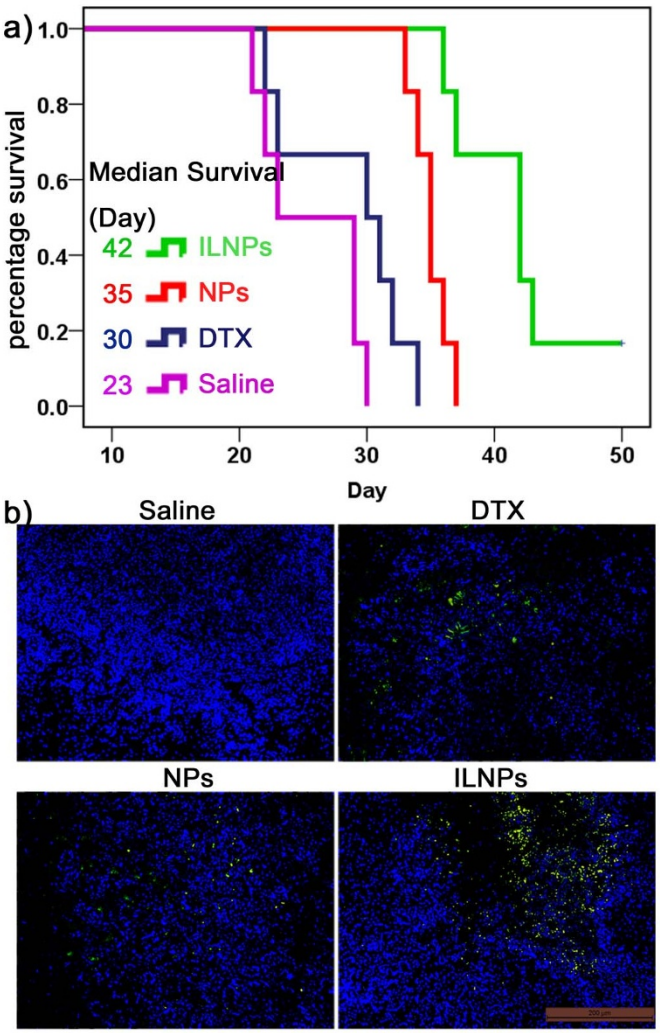

Figure 2 | Anti glioma effect of DTX-loaded ILNPs. (a) Cumulative survival study of glioma bearing mice treated with 10 mg/kg DTX, DTX-loaded NPs, DTX-loaded ILNPs or saline (n = 6). (b) Terminal deoxynucleotide transferase dUTP Nick End Labeling (TUNEL) assay of slices of glioma bearing brains from mice treated with different formulations. Blue represents nuclei, while green represents apoptosis cells. The scale bar represents 200 μm.

NPs (P = 0.001, 0.001, and 0.005, respectively). At the end of a 50-day long study, one mouse survived. Accordingly, glioma cells were widely apoptotic after treatment with DTX-loaded ILNPs, but only slight apoptosis occurred in gliomas from mice treated with DTX-loaded NPs or free DTX (Figure 2b).

Cellular uptake. IL-13Rα2 is a tumor-specific receptor overexpressed in glioma cells[12]. Our data also showed that IL-13Rα2 was overexpressed on U87 cells and C6 cells, and that it was expressed at low levels on macrophages (Raw246.7 cells) and endothelial cells (bEnd.3 and HUVEC) (Figure 1b). Thus, U87 cells and Raw246.7 cells were selected for the cellular uptake assay. The cellular uptake of nanoparticles was concentration- and time- dependent (Figure 3). As the nanoparticle concentration increased, the uptake increased in both the NP and ILNP group (Figure 3a). At an equal dose, the ILNPs were taken up by U87 cells at greater levels than NPs. However, the uptake of ILNPs by Raw246.7 cells (a macrophage cell line) was almost the same as that of NPs. The uptake ratio of ILNPs/NPs by U87 cells increased to over 1.4 at nanoparticles concentrations of 200 μg/mL and 800 μg/mL, while the uptake ratio by Raw246.7 cells was almost 1.0 (Figure 3c), suggesting that conjugation with the IL-13 peptide selectively increased the targeting of nanoparticles to glioma cells rather than macrophage cells. Similarly, increasing the incubation time also enhanced the uptake of NPs and ILNPs by both U87 and Raw246.7 cells (Figure 3b). However, the ILNPs/NPs uptake ratio by U87 cells decreased with time (Figure 3d), indicating that a long incubation time could enhance non-specific uptake.

Intracellular localization. The internalization mechanisms and intracellular trafficking of nanoparticles requires further study, especially regarding the difference between targeted and non-targeted nanoparticles. Thus, this study examined the intracellular localization and subsequently the uptake mechanisms and intercellular trafficking. After 30-min incubation, the uptake of ILNPs by U87 cells was higher than that of NPs. ILNPs were distributed throughout the whole cell; however, the NPs were mostly co-localized with the endosomes, which were marked by LysoTracker Red, indicating that the cellular uptake was associated with the endosomes and modification with IL-13 peptide facilitated the transportation of nanoparticles into cytoplasm (Figure 3e). After a 2-h incubation, the cellular uptake of ILNPs was still higher than that of NPs, while the colocalization of NPs with endosomes decreased and the fluorescence of NPs was dispersed throughout the whole cell, suggesting that the ILNPs might escape from the endosomes into the cytoplasm or be resorted to other organelles during the 2-h incubation (Figure 3f).

Cellular uptake mechanisms and intercellular trafficking. Endocytosis is the main pathway by which these nanoparticles were taken up into cells. Inhibitors and the response of NPs and ILNPs to the inhibitors were elucidated in Table 1. Cellular uptake of ILNPs and NPs by U87 cells was through energy-dependent endocytosis, as it was reduced to 78.0% and 82.4% of the control after energy depletion by sodium azide, respectively (Figure 4a). In addition, the endocytosis inhibitor phenylarsine oxide greatly reduced the cellular uptake of ILNPs and NPs to 40.8% and 51.5% respectively, suggesting that endocytosis was involved in both the ILNPs and the NPs uptake. Endocytosis involves at least four basic mechanisms: caveolae-mediated endocytosis, clathrin-mediated endocytosis, macropinocytosis and clathrin and caveolae-independent endocytosis[18,19]. Clathrin-mediated endocytosis, used by all eukaryotic cells to internalize nutrients and degrade or recycle substances, is well-known for its role in the selective uptake of molecules through specific receptors[20]. Sucrose and chlorpromazine, blocking agents of clathrin-coated pit formation[19], considerably decreased the ILNPs uptake to 25.2% and 61.3%, respectively, indicating the involvement of clathrin-mediated endocytosis in ILNPs uptake. However, the sucrose and chlorpromazine only decreased the NPs uptake to 52.9% and 95.7%, respectively, which were considerably higher than the uptake for the ILNPs, suggesting the clathrin-mediated endocytosis was more important for the uptake of ILNPs than for that of NPs. Filipin, a special inhibitor of caveolae-associated endocytosis[21], significantly (P = 0.003) decreased the ILNPs uptake, while it had no significant inhibition effect on the NPs uptake, indicating that caveolae-associated endocytosis was involved in the ILNPs uptake but not in the NPs uptake. Nocodazole, an inhibitor of macropinocytosis, and cytochalasin D, microtubule-disrupting agents[22], significantly (P = 0.0006) decreased the uptake of NPs to 71.9% and 61.4%, while they only decreased the uptake of ILNPs to

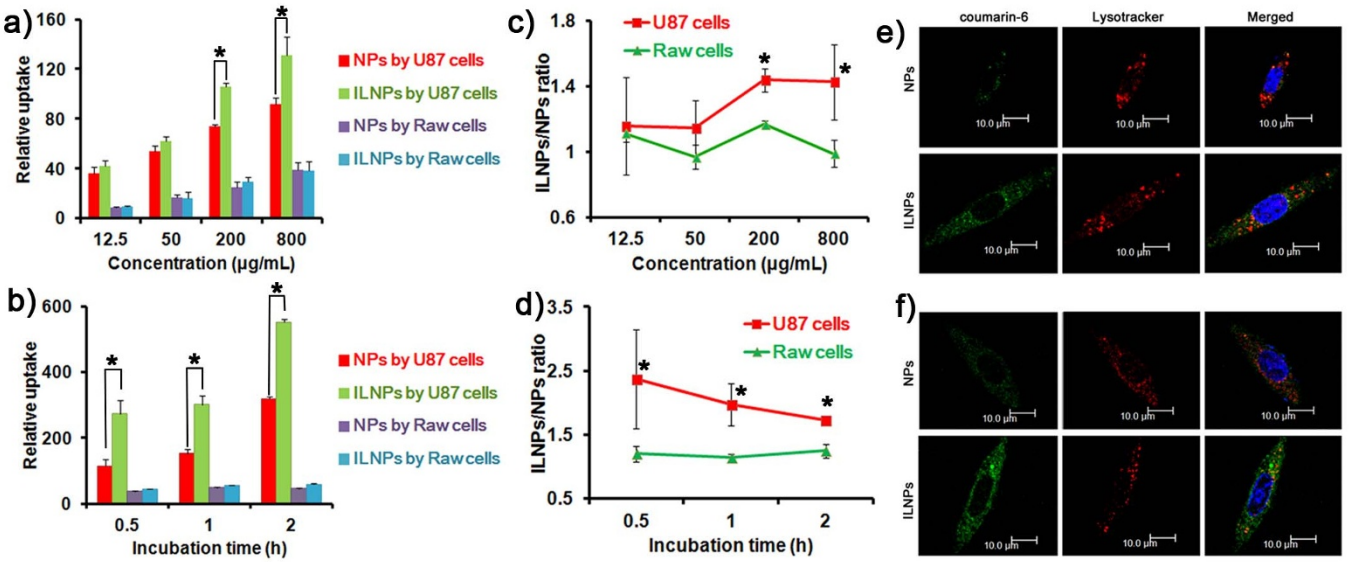

Figure 3 | Cellular uptake of ILNPs. (a) and (c) *In vitro* cellular uptake of different concentrations of coumarin-6-loaded NPs or ILNPs for 1 h. (b) and (d) Cellular uptake of 200 μg/mL coumarin-6-loaded NPs or ILNPs for different times. (e) Intracellular localization of coumarin-6-loaded NPs and ILNPs incubated with U87 cells for 0.5 h. (f) Intracellular localization of coumarin-6-loaded NPs and ILNPs incubated with U87 cells for 2 h. The nuclei were stained with DAPI and the endosomes were marked with LysoTracker Red.

Table 1 | The function of different inhibitors and the response of NPs and ILNPs to these inhibitors

Inhibitors	Function	NPs	ILNPs
Sodium azide	Energy	+	+
Phenylarsine oxide	Endocytosis	++	++
Sucrose	Blocking agents of clathrin-coated pit formation	+	++
chlorpromazine	Blocking agents of clathrin-coated pit formation	−	++
Nocodazole	Inhibitor of macropinocytosis	+	−
Cytochalsin D	Microtubule-disrupting agent	++	+
Filipin	Inhibitor of caveolae-associated endocytosis	−	+
BFA	Disrupture of Golgi apparatus	−	+
Monensin	lysosome inhibitor	−	+

"+" means positive response to the inhibitors, "++" means greatly positive response to the inhibitors, "−" means negative response to the inhibitors.

90.2% and 63.6%, suggesting that macropinocytosis was more important for NPs uptake than for ILNPs uptake. The Golgi apparatus and lysosomes have important roles in both intracellular cargo transport and disposition[23,24]. In this study, brefeldin A (BFA), which disrupts the Golgi apparatus, significantly ($P = 0.028$) decreased the uptake of ILNPs rather than NPs, suggesting the involvement of the Golgi apparatus in the intracellular transport of ILNPs. Although the lysosome inhibitor monensin considerably decreased the uptake of ILNPs and NPs, the uptake of ILNPs was obviously lower than that of NPs, indicating that lysosomes are involved in the intracellular transport of both ILNPs and NPs.

To more precisely determine the main uptake pathway, different concentrations of chlorpromazine, nocodazole and cytochalasin D were used in the uptake inhibition study. Although both 5 μg/mL and 20 μg/mL chlorpromazine could significantly inhibit the uptake of ILNPs and NPs, the relative uptake of ILNPs was much lower than that of NPs (Figure 4b). At the same time, the relative uptake of ILNPs in the presence of sucrose was considerably lower than that of NPs, suggesting that clathrin-mediated endocytosis was a more important endocytosis pathway for ILNPs than for NPs. On the contrary, nocodazole and cytochalasin D inhibited the uptake of NPs to a greater extent than that of ILNPs (Figure 4c). The uptake inhibition by 50 μM nocodazole was considerably stronger for NPs than for ILNPs. Cytochalasin D, even at concentrations as low as 2.5 μM, could considerably decrease the uptake of NPs rather than ILNPs. These results suggested that macropinocytosis was a more important pathway for NPs uptake than for ILNPs uptake.

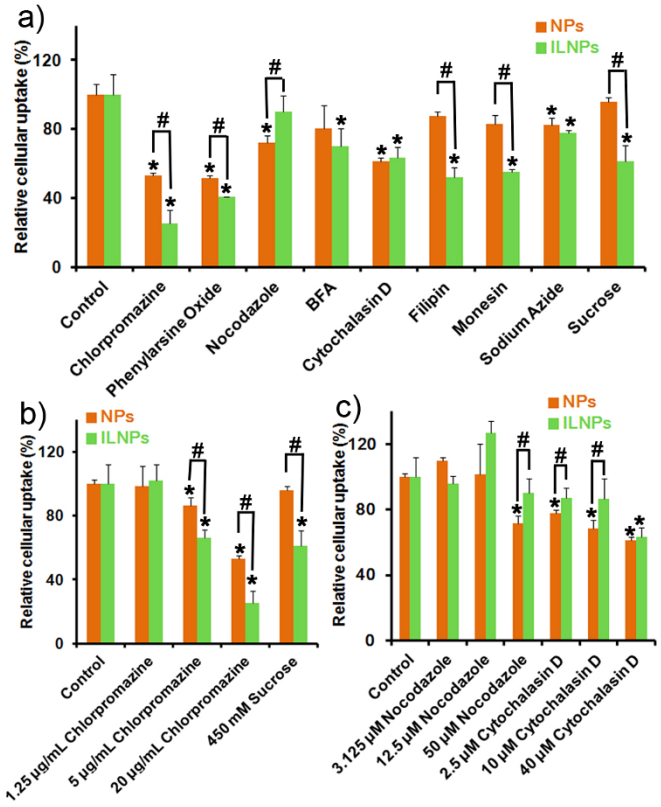

Figure 4 | Mechanisms of uptake of NPs and ILNPs by U87 cells. Cells were treated with 200 μg/mL coumarin-6-loaded ILNPs of NPs for 1 h in the presence of various inhibitors (a), different concentrations of chlorpromazine and sucrose (b), and different concentrations of nocodazole and Cytochalasin D (c). The uptake was presented as percentage of the control (n = 3). $*p < 0.05$ vs control, $^{\#}p < 0.05$ between NPs and ILNPs.

***In vitro* cellular internalization visualized by TEM.** According to the uptake inhibition study, several pathways were involved in the endocytosis procedure of nanoparticles. To clearly identify these pathways, TEM was utilized to capture these procedures, and SPIO was used to track the ILNPs. Several pathways were captured (Figure 5). SPIO can be observed in the gaps between cells, or be internalized into cells and in cell endosomes. Some typical macropinosomes had already been formed (Figure 5a) or was beginning to form (Figure 5h, e), which directly demonstrated the involvement of macropinocytosis. Clathrin-dependent pinocytosis and receptor-mediated endocytosis can form pits, as can be observed in Figure 5b. However, the pit could not be identified as clathrin-dependent or receptor-mediated. Some SPIOs-loaded ILNPs were captured in the phagosome (Figure 5g, i), suggesting that the ILNPs uptake involved phagocytosis.

***In vivo* imaging.** Controversy exists regarding the function of targeting ligands. Most results have shown increased accumulation in the tumor site when NPs are functionalized with tumor targeting ligands, while some results have shown no difference between ligand modified NPs and unmodified NPs[6]. However, modification with targeting ligands indeed increased the internalization into tumor cells[25]. *In vivo* imaging is a powerful method that indicates *in situ* whole body distribution of dye-loaded particles during a period of time[26,27]. To confirm the targeting effect *in vivo*, the whole body distribution of DiR-loaded NPs and ILNPs was determined by *in vivo* imaging (Figure 6). ILNPs were specifically targeted to gliomas with greater efficiency than NPs. ILNPs and NPs were both located in the glioma bed as confirmed by 3D reconstruction (Video S1 and Video S2). The superior glioma targeting efficiency of ILNPs was further demonstrated by *ex vivo* imaging of the brain (Figure 6c, d). The intensity in normal brain was almost the same between NPs and ILNPs, but the intensity of ILNPs in the glioma was 3.81-fold higher than that of NPs. However, both NPs and ILNPs could distribute into normal tissues without significant difference, which might cause side effects.

Tissue distribution. To further elucidate the distribution of NPs and ILNPs in glioma bearing brains, frozen sections were prepared. The ILNPs and NPs exhibited different distributions in the tumor site (Figure 7). ILNPs were present in the tumor at much higher levels than NPs, consistent with the *in vivo* imaging study. Macrophages and microvessels were stained to accurately elucidate the distribution in the glioma site. There was no obvious difference between NPs and ILNPs in colocalization with macrophages (Figure 7a) and microvessels (Figure 7b). In contrast, ILNPs showed good colocalization with glioma cells, suggesting that conjugation with the IL-13 peptide

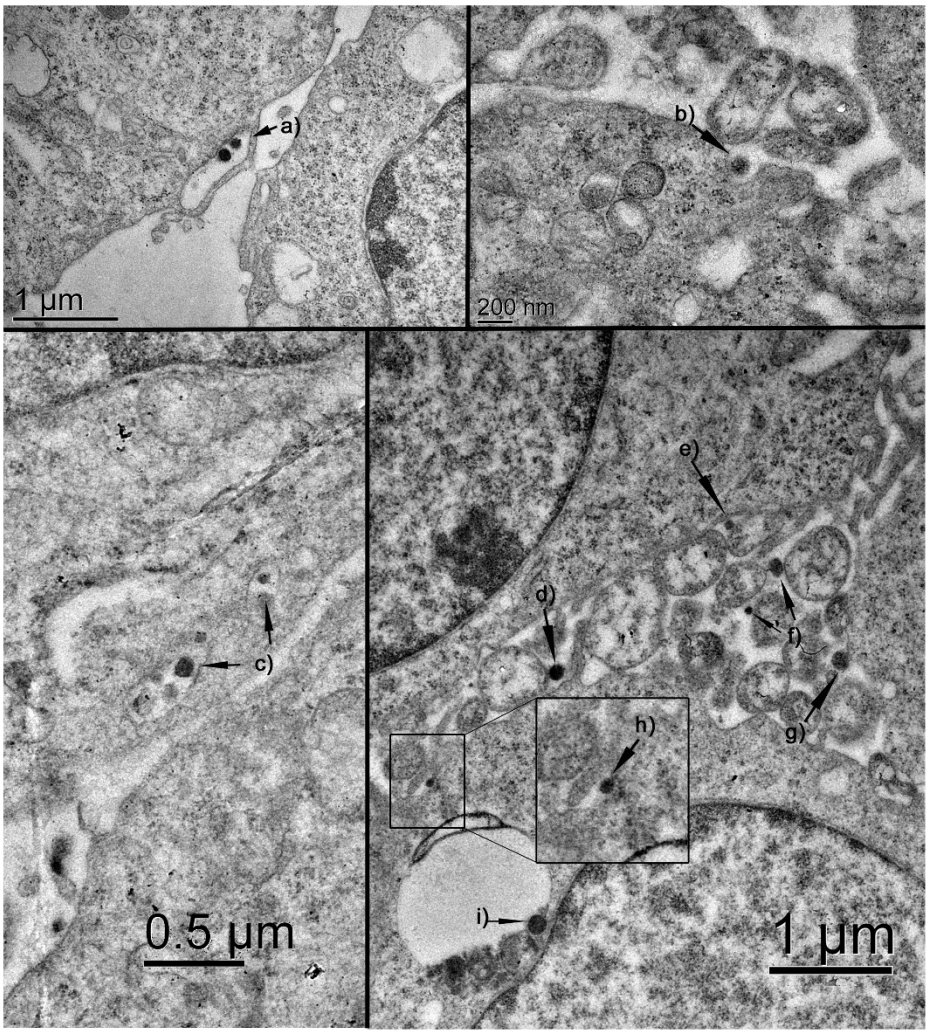

Figure 5 | ***In vitro*** **internalization of ILNPs.** The SPIO-loaded ILNPs were observed internalized near the cell membrane, mediated by clathrin-dependent pinocytosis or receptor-mediated endocytosis (b), macropinocytosis (h and e), clathrin-independent pinocytosis (d) or phagocytosis (g). SPIO-loaded ILNPs were also observed in the gaps between cells (f), in the macropinosomes mediated by macropinocytosis (a), in the phagosomes mediated by phagocytosis (i) and in the endosomes (c).

enhanced the internalization of nanoparticles by glioma cells rather than other cells in the glioma bed.

Discussion

In this study, an *in vivo* glioma bearing mice survival study and a glioma apoptosis experiment were carried out to determine the effects of targeting ligands modification to nanoparticles on glioma management. DTX-ILNPs exhibited significantly better anti-glioma activities than DTX-NPs, DTX and saline. These effects were consistent with many other studies showing that modification with glioma targeting ligands improved the anti-glioma efficiency of drug-loaded systems[27–30]. Thus, NPs and ILNPs could be utilized to elucidate the function of glioma targeting ligand modification.

In vitro cellular uptake demonstrated that conjugation with the IL-13 peptide selectively increased the targeting to glioma cells rather than macrophage cells, making them useful for enhanced glioma treatment. However, the ILNPs/NPs uptake ratio by U87 cells decreased when the incubation time increased, indicating that a long incubation time could enhance non-specific uptake and reduce the difference in cellular uptake between targeted and non-targeted nanoparticles, and it was consistent with previous results[31]. These results demonstrated that modification with targeting ligands facilitated nanoparticles uptake by target cells but exhibited no effect on non-target cells, which was in good agreement with other studies[16,32]. The selective targeting effect of ILNPs to glioma cells was further evaluated by intracellular location study. It indicated that modification with the IL-13 peptide could facilitate the internalization process, leading to more rapid distribution of nanoparticles throughout the cytoplasm. The increased endosomal escape after nanoparticle modification with targeting ligands has also been demonstrated by many other studies[21,33,34], and this may explain why targeting ligand modification increased the cellular uptake of nanoparticles. It was pointed out that receptor ubiquitination could trigger the clathrin-coated pit scission from the membrane and complete the endocytic procedure[35]. Preubiquitinated epidermal growth factor receptor (EGFR) and ErbB2 could be constitutively endocytosed into cells[36,37]. Thus, the interaction between targeting ligands and receptors may induce the ubiquitination of receptors, leading to a rapid endocytosis of ligand-modified nanoparticles. However, this hypothesis need to be further explored.

Although several pathways participated into the uptake procedures of both NPs and ILNPs, it should be noted that the conjugation of the IL-13 peptide to nanoparticles could change the main uptake pathway from macropinocytosis to clathrin-mediated endocytosis. This may because the conjugation with IL-13 peptide considerably increased the uptake rate through IL13Rα2-mediated endocytosis,

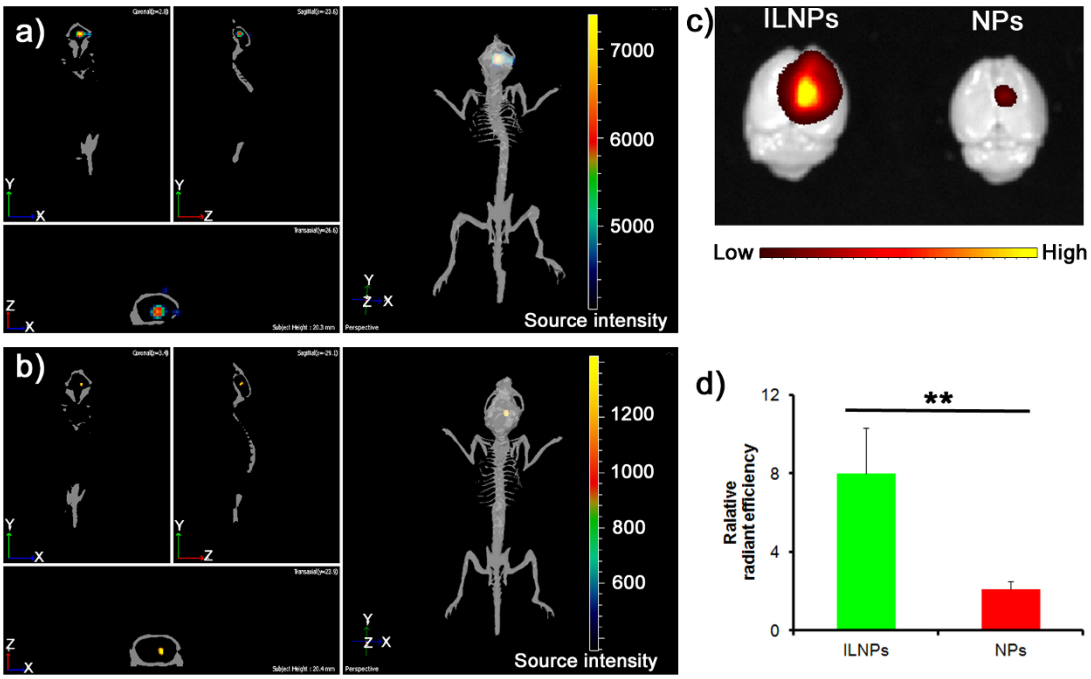

Figure 6 | *In vivo* and *ex vivo* imaging. (a) Fluorescent imaging of glioma bearing mice 2 h after administered DiR-loaded ILNPs. (b) Fluorescent imaging of glioma bearing mice 2 h after administration of DiR-loaded NPs. (c) *Ex vivo* imaging of brains 2 h after administration of DiR-loaded ILNPs and NPs. (d) Semi-quantitative results of fluorescence intensity of gliomas, $^{**}p < 0.01$ *vs* control.

which was demonstrated by the intracellular localization study. These results are consistent with other studies showing that the endocytosis pathway differs between target and non-target cells[38]. However, inconsistent data have also been published in this field

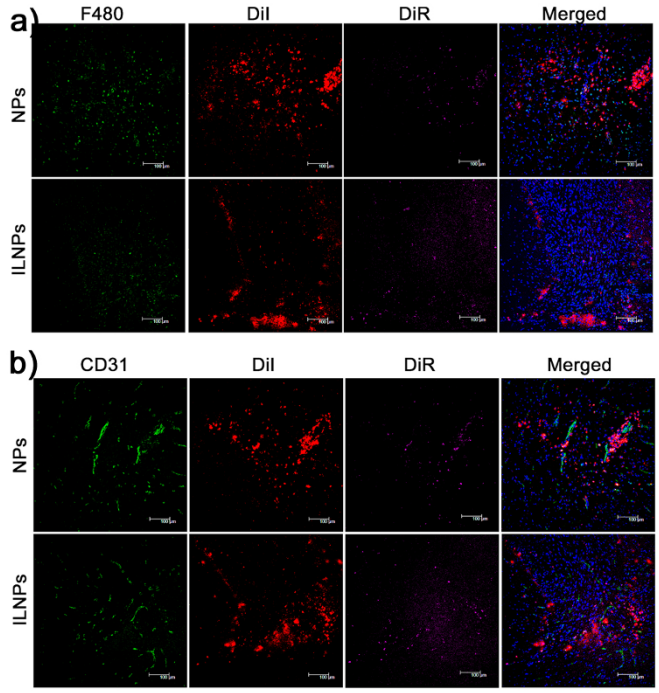

Figure 7 | Brain glioma distribution of DiR-loaded ILNPs. (a) The colocalization of ILNPs with macrophages stained with anti-F4/80 antibody. (b) The colocalization of ILNPs with microvessels stained with anti-CD31 antibody. Blue represents nuclei stained by DAPI, green are macrophages (a) or microvessels (b), red are glioma cells pre-stained by DiI, pink are DiR-loaded NPs or ILNPs, and the scale bar represents 100 μm.

(see Supplementary Table S2 online for the uptake mechanisms of several targeted NPs). Clathrin-mediated endocytosis is a pathway involved in many proteins, which possess different roles in the endocytosis procedure. Selective knockdown the expression of specific proteins resulted in different influences on the clathrin-mediated endocytosis of different receptors[39]. For example, knockdowning clathrin heavy chain and dynamin produced maximal inhibitory effects on the internalization of both EGFR and transferrin receptors while clathrin-assembly lymphoid myeloid leukemia protein did not influence transferrin endocytosis but considerably affected EGFR internalization. As demonstrated in this study, ligands modification on nanoparticles could change the main endocytosis pathway from macropinocytosis to clathrin-mediated endocytosis. However, it is not clear that the clathrin-mediated endocytosis of ligand-modified nanoparticles is similar or different from the endocytosis of free ligands, which is interesting and needs further investigation. The results will be useful for the selection of conjugation methods of ligands onto nanoparticles.

The *in vivo* distribution data forcefully demonstrated that modification with the IL-13 peptide could increase the glioma localization of nanoparticles, which was in agreement with many previous reports[14,27,28,31]. However, most reports have only demonstrated enhanced distribution to the glioma by targeted delivery, while the localization of the nanoparticles in various cell types was not clear[16,40]. Similar to uptake by Raw246.7 cells, there was no obvious difference between NPs and ILNPs in colocalization with macrophages, suggesting that modification with the IL-13 peptide did not alter the distribution in non-target cells. The colocalization with microvessels also showed no significant difference between NPs and ILNPs, indicating that the increased localization in the tumor was not caused by adhesion onto/into microvessels. These results are likely due to the low expression of IL-13Rα2 on macrophages and endothelial cells. In contrast, ILNPs showed good colocalization with glioma cells, suggesting that conjugation with the IL-13 peptide enhanced the internalization by glioma cells rather than other cells in the glioma bed. The increased internalization might be caused by IL-13Rα2-mediated endocytosis, which was demonstrated by *in vitro*

cellular uptake. Combining these results, we concluded that IL-13 peptide modification increased rapid internalization by glioma cells and thus led to a greater distribution of ILNPs into the glioma bed from the blood circulation by the EPR effect.

This study provides the information about the function of ligands modification on nanoparticles, which is useful for the design of effective targeting delivery systems. However, the interaction between NPs and biological fluid/membranes occurs as soon as the NPs are introduced into a biological system and a protein corona would be formed[41]. Although many papers have been published regarding the use of various ligands to improve targeting effects and promising results have been provided, most *in vitro* studies (including this study) were performed free of serum. Modification with ligands may alter the interactions between NPs and serum protein and have a concessive effect on the interaction between NPs and cells, the blood circulation time of NPs, and their *in vivo* targeting effect. Thus, further studies need be carried out to elucidate the interaction between serum protein and targeting ligands, which is essential for optimizing the targeting delivery system.

In conclusion, conjugation with the glioma targeting IL-13 peptide selectively increased nanoparticles uptake and internalization by glioma cells rather than macrophage cells. The addition of the IL-13 peptide to nanoparticles clearly increased the cellular uptake mediated by clathrin-depended endocytosis, while the dominant uptake pathway for unmodified NPs is macrophagocytosis. However, only quantitative changes were observed in the uptake pathways, with most pathways active in both ILNPs and NPs uptake. *In vivo* experiments revealed that the modification with the IL-13 peptide significantly increased the distribution of nanoparticles in the glioma site and the increased delivery to the glioma was caused by elevated internalization by glioma cells rather than by macrophages or microvessels.

Methods

Materials. IL-13 peptide was synthesized by Chinapeptide (Shanghai, China). DTX was purchased from Knowshine (Shanghai, China). Methoxy poly(ethyleneglycol)-poly(ε-caprolactone) (MPEG-PCL)(Mw: 3 k–15 k) and carboxyl poly(ethylene glycol)-poly(ε-caprolactone) (HOOC-PEG-PCL)(Mw: 3.4 k–15 k) were synthesized as previously described[42].

BALB/c nude mice (male, 4–5 weeks, 18–22 g) were obtained from the Shanghai Slac Laboratory Animal Co, Ltd. (Shanghai, China) and maintained under standard housing conditions. All animal experiments were carried out in accordance with protocols evaluated and approved by the ethics committee of Fudan University.

Preparation and characterization of NPs. The PEG-PCL NPs were prepared by a previously described emulsion/solvent evaporation method[16]. Briefly, 28 mg of MPEG-PCL and 2 mg of HOOC-PEG-PCL were dissolved in 1 mL of dichloromethane and then added into 5 mL of a 0.6% sodium cholate hydrate solution. The mixture was then pulse sonicated for 75 s at 200 W on ice using a probe sonicator (Scientz Biotechnology Co. Ltd., China). Then, the emulsion was applied to a rotary evaporator to remove the dichloromethane and the NPs were condensed to a fixed concentration by ultrafiltration at 4,000 *g*.

For the IL-13 peptide conjugation (ILNPs), the carboxyl units of NPs were activated by EDC and NHS in a pH 6.0 MES buffer for 0.5 h. The MES buffer was then replaced by phosphate-buffered saline (PBS) (pH 7.4) using a Hitrap™ desalting column, and 50 μg of IL-13 peptide in 1 mL of PBS (pH 7.4) was added into the NPs suspension and stirred for 4 h in the dark. The product was then subjected to ultrafiltration to remove the unconjugated IL-13 peptide, and the nanoparticles were collected. SPIO-, coumarin-6- and DiR-loaded ILNPs were prepared using the same procedure except that the materials were dissolved in 1 mL of dichloromethane, which contained SPIO, coumarin-6 or DiR.

The particle sizes and Zeta potentials were determined by a Malvern Zeta Sizer (Malvern, NanoZS, UK). The ILNPs morphology was carried examined by TEM after staining with 2% (w/v) phosphotungstic acid solution.

The stability of the NPs and ILNPs was evaluated in PBS and FBS. NPs and ILNPs were suspended in PBS (pH 5.0 and pH 7.4) at 0.2 mg/mL in a 37°C shaker. The particle size and PDI were measured every day for 7 days. To evaluate the stability in FBS, NPs and ILNPs were suspended in PBS (pH 7.4) supplemented with FBS (0%, 50% and 90%). Then 0.2 mg/mL NPs and ILNPs were incubated in a 37°C shaker. The absorbance of the NPs and ILNPs at 560 nm was measured at preset time points.

Anti-glioma effect. Glioma bearing mice were established as described previously[43]. Mice were anesthetized and fixed on a stereotaxic apparatus. A 5 μL suspension containing 5×10^5 U87 cells was slowly injected into the right corpus striatum of the nude mice. Eight days post implantation, mice were randomly divided into four groups (9 mice for each group): saline, DTX, NPs and ILNPs. Mice received four injections of 10 mg/kg DTX in different formulations or an equal volume of saline every three days. The survival time of the mice was recorded and analyzed by IBM SPSS 19.0. On the 20th day after cell injection, three mice in each group were chosen randomly to determine the glioma cell apoptosis.

Cellular uptake. U87 glioma cells and Raw246.7 cells in the logarithmic growth phase were seeded on 24-well plates at a density of 1×10^4 cells/mL. Twenty four hours later, different concentrations of coumarin-6-loaded NPs or ILNPs were added into the wells and incubated for different periods of time. The adsorptive and free particles were removed by washing with ice-cold PBS and acid buffer [120 mmol/L NaCl, 20 mmol/L sodium barbital, 20 mmol/L sodium acetate (pH 3)] at 4°C for 5 min, followed by ice-cold PBS. To quantitatively determine the fluorescence intensity, the cells were digested and detected by a FACS Aria Cell Sorter (BD, USA).

Intracellular localization. U87 cells were seeded in glass-bottom dishes at a density of 1×10^4 cells/mL and incubated at 37°C for 24 h. After a 5-min incubation in PBS, the cells were treated for 30 min or 120 min with 200 μg/mL coumarin-6 loaded NPs or ILNPs. Thirty minutes before the incubation ended, Lysotracker Red DND-99 (50 nmol/L), a marker of endolysosomal compartments, was added into the wells. After nuclear staining with DAPI (1 μg/mL) for 5 min, the cells were washed, fixed and mounted in fluorescent mounting medium. Images were captured with a confocal microscope (TCS SP5, Leica, Germany) and were superimposed to determine the intracellular localization of the nanoparticles.

Cellular uptake mechanism. U87 cells were seeded in 6-well plates at a density of 2×10^5 cells/mL and incubated for 48 h. After a 20-min pre-incubation in DMEM, the cells were treated with 200 μg/mL of coumarin-6-loaded NPs or ILNPs and various inhibitors for 1 h respectively: PBS (control), 20 μg/mL chlorpromazine, 2 μmol/L phenylarsine oxide, 10 μg/mL filipin, 40 μmol/L cytochalasin D, 450 mmol/L sucrose, 0.1% w/v sodium azide, 200 nmol/L monensin, 50 μmol/L nacodazole, 20 μg/mL BFA. After washing with ice-cold PBS, acid buffer [120 mmol/L NaCl, 20 mmol/L sodium barbital, 20 mmol/L sodium acetate (pH 3)] at 4°C for 5 min and ice-cold PBS, the cells were digested and the mean fluorescence intensity was observed by flow cytometry (FACS Aria Cell Sorter, BD, USA). To more precisely determine the involvement of clathrin-mediated endocytosis and macropinocytosis, U87 cells in 6-well plates were treated with coumarin-6-loaded NPs or ILNPs in the presence of inhibitors with different concentrations: 1.25, 5 or 20 μg/mL chlorpromazine, 450 mmol/L sucrose, 2.5, 10 or 40 μmol/L cytochalasin D or 3.125, 12.5 or 50 μmol/L nocodazole. After 1 h incubation, cells were handled as described above.

***In vitro* internalization.** U87 cells were seeded in the 10 cm dishes at a density of 1×10^5 cells/mL. After 24 h incubation, cells were treated with 500 μg/mL SPIO-loaded ILNPs for 1 h. The cells were directly harvested with a cell scraper and centrifuged at 2500 rpm for 10 min. After fixation by a 2.5% glutaraldehyde solution, the cells were embedded in an epoxy resin, cut into ultra-thin sections with an ultramicrotome using a diamond knife, and mounted on 150 mesh copper grids. The cell ultrastructures were stained with uranyl acetate and lead citrate and then observed under TEM.

***In vivo* imaging.** The glioma bearing mice were established as described above. Ten days later, 2 mg/kg of DiR-loaded NPs or ILNPs were injected into the GBM bearing mice. The distribution of fluorescence was observed by an IVIS spectrum *in vivo* imaging system (Caliper, MA, USA) 2 h post injection. Mice were sacrificed at 2 h and the *ex vivo* image of the brain was also captured at that time.

Brain distribution. The DiR-loaded NPs were used to investigate the *in vivo* distribution of NPs in mice bearing U87 orthotopic glioma as described above, except that the U87 cells were prestained with 10 μmol/L DiI for 20 min at 37°C. Twelve days after tumor implantation, the DiR-loaded ILNPs or NPs were *i.v.* administered to the mice. After 2 h, the mice were anesthetized and the hearts were perfused with saline followed by 4% paraformaldehyde. The brain was removed for consecutive frozen sections of 5 μm thicknesses preparation. Macrophages were stained with anti-F4/80 antibody and microvessels were stained with anti-CD31 antibody. The distribution of fluorescence was observed by a confocal microscope (TCS SP5, Leica, Germany).

Statistic analysis. Data were presented as mean ± SD. Statistical differences in cell uptake and *in vivo* imaging were determined by student t test. The probability of survival was determined by the Kaplan-Meier method and compared by the log-rank test.

1. Matsumura, Y. & Maeda, H. A new concept for macromolecular therapeutics in cancer chemotherapy: mechanism of tumoritropic accumulation of proteins and the antitumor agent smancs. *Cancer Res* **46**, 6387–92 (1986).
2. Jain, R. K. Delivery of molecular and cellular medicine to solid tumors. *Adv Drug Deliv Rev* **46**, 149–68 (2001).

3. Mickler, F. M. *et al.* Tuning Nanoparticle Uptake: Live-Cell Imaging Reveals Two Distinct Endocytosis Mechanisms Mediated by Natural and Artificial EGFR Targeting Ligand. *Nano Lett* **12**, 3417–23 (2012).
4. Liu, Y. & Lu, W. Recent advances in brain tumor-targeted nano-drug delivery systems. *Expert Opin Drug Deliv* **9**, 671–86 (2012).
5. Bae, Y. H. & Park, K. Targeted drug delivery to tumors: myths, reality and possibility. *J Control Release* **153**, 198–205 (2011).
6. Choi, C. H., Alabi, C. A., Webster, P. & Davis, M. E. Mechanism of active targeting in solid tumors with transferrin-containing gold nanoparticles. *Proc Natl Acad Sci U S A* **107**, 1235–40 (2010).
7. Ashley, C. E. *et al.* The targeted delivery of multicomponent cargos to cancer cells by nanoporous particle-supported lipid bilayers. *Nat Mater* **10**, 389–97 (2011).
8. Florence, A. T. "Targeting" nanoparticles: the constraints of physical laws and physical barriers. *J Control Release* **164**, 115–24 (2012).
9. Agarwal, S., Sane, R., Oberoi, R., Ohlfest, J. R. & Elmquist, W. F. Delivery of molecularly targeted therapy to malignant glioma, a disease of the whole brain. *Expert Rev Mol Med* **13**, e17 (2011).
10. Shi, J., Xiao, Z., Kamaly, N. & Farokhzad, O. C. Self-assembled targeted nanoparticles: evolution of technologies and bench to bedside translation. *Acc Chem Res* **44**, 1123–34 (2011).
11. Pirollo, K. F. & Chang, E. H. Does a targeting ligand influence nanoparticle tumor localization or uptake? *Trends Biotechnol* **26**, 552–8 (2008).
12. Mintz, A., Gibo, D. M., Slagle-Webb, B., Christensen, N. D. & Debinski, W. IL-13Ralpha2 is a glioma-restricted receptor for interleukin-13. *Neoplasia* **4**, 388–99 (2002).
13. Kawakami, M., Leland, P., Kawakami, K. & Puri, R. K. Mutation and functional analysis of IL-13 receptors in human malignant glioma cells. *Oncol Res* **12**, 459–67 (2001).
14. Fillmore, H. L. *et al.* Conjugation of functionalized gadolinium metallofullerenes with IL-13 peptides for targeting and imaging glial tumors. *Nanomedicine (Lond)* **6**, 449–58 (2011).
15. Shultz, M. D. *et al.* Encapsulation of a radiolabeled cluster inside a fullerene cage, (177)Lu(x)Lu((3−x))N@C(80): an interleukin-13-conjugated radiolabeled metallofullerene platform. *J Am Chem Soc* **132**, 4980–1 (2010).
16. Gao, H. *et al.* Precise glioma targeting of and penetration by aptamer and peptide dual-functioned nanoparticles. *Biomaterials* **33**, 5115–23 (2012).
17. Wang, Y. *et al.* Multifunctional mesoporous silica-coated graphene nanosheet used for chemo-photothermal synergistic targeted therapy of glioma. *J Am Chem Soc* **135**, 4799–804 (2013).
18. Liu, J. & Shapiro, J. I. Endocytosis and signal transduction: basic science update. *Biol Res Nurs* **5**, 117–28 (2003).
19. Xin, H. *et al.* Angiopep-conjugated poly(ethylene glycol)-co-poly(epsilon-caprolactone) nanoparticles as dual-targeting drug delivery system for brain glioma. *Biomaterials* **32**, 4293–305 (2011).
20. Mahmoudi, M., Azadmanesh, K., Shokrgozar, M. A., Journeay, W. S. & Laurent, S. Effect of nanoparticles on the cell life cycle. *Chem Rev* **111**, 3407-32 (2011).
21. Lu, W., Sun, Q., Wan, J., She, Z. & Jiang, X. G. Cationic albumin-conjugated pegylated nanoparticles allow gene delivery into brain tumors via intravenous administration. *Cancer Res* **66**, 11878–87 (2006).
22. Nam, H. Y. *et al.* Cellular uptake mechanism and intracellular fate of hydrophobically modified glycol chitosan nanoparticles. *J Control Release* **135**, 259–67 (2009).
23. Pang, Z. *et al.* Brain delivery and cellular internalization mechanisms for transferrin conjugated biodegradable polymersomes. *Int J Pharm* **415**, 284–92 (2011).
24. Jiang, S., Rhee, S. W., Gleeson, P. A. & Storrie, B. Capacity of the Golgi apparatus for cargo transport prior to complete assembly. *Mol Biol Cell* **17**, 4105–17 (2006).
25. Kirpotin, D. B. *et al.* Antibody targeting of long-circulating lipidic nanoparticles does not increase tumor localization but does increase internalization in animal models. *Cancer Res* **66**, 6732–40 (2006).
26. Pang, Z. *et al.* Lactoferrin-conjugated biodegradable polymersome holding doxorubicin and tetrandrine for chemotherapy of glioma rats. *Mol Pharm* **7**, 1995–2005 (2010).
27. Zhan, C. *et al.* Cyclic RGD conjugated poly(ethylene glycol)-co-poly(lactic acid) micelle enhances paclitaxel anti-glioblastoma effect. *J Control Release* **143**, 136–42 (2010).
28. Gu, G. *et al.* PEG-co-PCL nanoparticles modified with MMP-2/9 activatable low molecular weight protamine for enhanced targeted glioblastoma therapy. *Biomaterials* **34**, 196–208 (2013).
29. Guo, J. *et al.* Aptamer-functionalized PEG-PLGA nanoparticles for enhanced anti-glioma drug delivery. *Biomaterials* **32**, 8010–20 (2011).
30. Xin, H. *et al.* Anti-glioblastoma efficacy and safety of paclitaxel-loading Angiopep-conjugated dual targeting PEG-PCL nanoparticles. *Biomaterials* (2012).
31. Yan, H. *et al.* Two-Order Targeted Brain Tumor Imaging by Using an Optical/Paramagnetic Nanoprobe across the Blood Brain Barrier. *ACS Nano* **6**, 410–20 (2012).
32. Kibria, G., Hatakeyama, H., Ohga, N., Hida, K. & Harashima, H. Dual-ligand modification of PEGylated liposomes shows better cell selectivity and efficient gene delivery. *J Control Release* **153**, 141–8 (2011).
33. Ren, J. *et al.* The targeted delivery of anticancer drugs to brain glioma by PEGylated oxidized multi-walled carbon nanotubes modified with angiopep-2. *Biomaterials* **33**, 3324–33 (2012).
34. Qian, Y. *et al.* PEGylated poly(2-(dimethylamino) ethyl methacrylate)/DNA polyplex micelles decorated with phage-displayed TGN peptide for brain-targeted gene delivery. *Biomaterials* **34**, 2117–29 (2013).
35. Henry, A. G. *et al.* Regulation of endocytic clathrin dynamics by cargo ubiquitination. *Dev Cell* **23**, 519–32 (2012).
36. Vuong, T. T. *et al.* Preubiquitinated chimeric ErbB2 is constitutively endocytosed and subsequently degraded in lysosomes. *Exp Cell Res* **319**, 32–45 (2013).
37. Bertelsen, V. *et al.* A chimeric pre-ubiquitinated EGF receptor is constitutively endocytosed in a clathrin-dependent, but kinase-independent manner. *Traffic* **12**, 507–20 (2011).
38. Raoof, M., Mackeyev, Y., Cheney, M. A., Wilson, L. J. & Curley, S. A. Internalization of C60 fullerenes into cancer cells with accumulation in the nucleus via the nuclear pore complex. *Biomaterials* **33**, 2952–60 (2012).
39. Huang, F., Khvorova, A., Marshall, W. & Sorkin, A. Analysis of clathrin-mediated endocytosis of epidermal growth factor receptor by RNA interference. *J Biol Chem* **279**, 16657–61 (2004).
40. Sun, X. *et al.* Co-delivery of pEGFP-hTRAIL and paclitaxel to brain glioma mediated by an angiopep-conjugated liposome. *Biomaterials* **33**, 916–24 (2012).
41. Nel, A. E. *et al.* Understanding biophysicochemical interactions at the nano-bio interface. *Nat Mater* **8**, 543–57 (2009).
42. Pang, Z. *et al.* Preparation and brain delivery property of biodegradable polymersomes conjugated with OX26. *J Control Release* **128**, 120–127 (2008).
43. Jones-Bolin, S., Zhao, H., Hunter, K., Klein-Szanto, A. & Ruggeri, B. The effects of the oral, pan-VEGF-R kinase inhibitor CEP-7055 and chemotherapy in orthotopic models of glioblastoma and colon carcinoma in mice. *Mol Cancer Ther* **5**, 1744–53 (2006).

Acknowledgements

We thank Professor Yalin Huang (Institutes of Biomedical Sciences, Fudan University) for technical assistance with confocal microscopy. We acknowledge support from the Biomedical Core Facility, Fudan University. This work was supported by the National Basic Research Program of China (973 Program, 2013CB932502), National Science and Technology Major Project (2012ZX09304004), National Natural Science Foundation of China (81001404) and the talent teacher program of Fudan University.

Author contributions

H.G., Z.P. and X.J. conceived the experiment, designed the project and wrote the paper. H.G. performed the experiments with the assistance of Z.Y., S.Z., S.C. and S.S.

Additional information

Supplementary information accompanies this paper at http://www.nature.com/scientificreports

Competing financial interests: The authors declare no competing financial interests.

How to cite this article: Gao, H.L. *et al.* Ligand modified nanoparticles increases cell uptake, alters endocytosis and elevates glioma distribution and internalization. *Sci. Rep.* **3**, 2534; DOI:10.1038/srep02534 (2013).

SCIENTIFIC REPORTS

DOI: 10.1038/srep05138

SUBJECT AREAS:
DRUG DELIVERY
CNS CANCER
BIOMEDICAL MATERIALS
CANCER MICROENVIRONMENT

SCIENTIFIC REPORTS:
3 : 2534
DOI: 10.1038/srep02534
(2013)

Published:
28 August 2013

Updated:
19 November 2014

CORRIGENDUM: Ligand modified nanoparticles increases cell uptake, alters endocytosis and elevates glioma distribution and internalization

Huile Gao, Zhi Yang, Shuang Zhang, Shijie Cao, Shun Shen, Zhiqing Pang & Xinguo Jiang

There is an error in Figure S2A found in the Supplementary Information of this Article. A TEM image of nanoparticles (NPs) is shown, instead of a TEM image of Interleukin 13 conjugated NPs (ILNPs). The correct Figure S2A appears below as Figure 1.

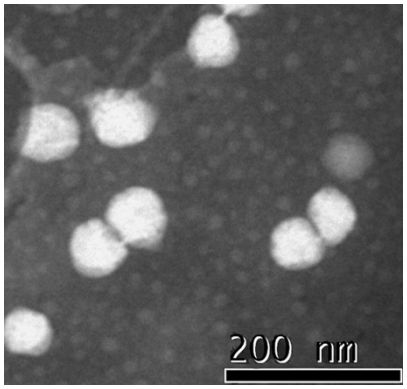

Figure 1 |